Taylor & Francis
Taylor & Francis Group

Transactions of the Indian Ceramic Society

ISSN: (Print) (Online) Journal homepage: https://www.tandfonline.com/loi/tcer20

# Effect of Zr/Ti Ratio on Piezoelectric and Dielectric Propertiesof $0.1Pb[Fe_{1/2}Nb_{1/2}]O_3$-$0.9Pb[Zr_xTi_{(1-x)}]O_{30}$ Ceramics

**Louanes Hamzioui, Fares Kahoul, Abdrazek Guemache, Michel Aillerie & Ahmed Boutarfaia**

**To cite this article:** Louanes Hamzioui, Fares Kahoul, Abdrazek Guemache, Michel Aillerie & Ahmed Boutarfaia (2021) Effect of Zr/Ti Ratio on Piezoelectric and Dielectric Propertiesof $0.1Pb[Fe_{1/2}Nb_{1/2}]O_3$-$0.9Pb[Zr_xTi_{(1-x)}]O_{30}$ Ceramics, Transactions of the Indian Ceramic Society, 80:1, 60-63, DOI: 10.1080/0371750X.2021.1871647

**To link to this article:** https://doi.org/10.1080/0371750X.2021.1871647

Published online: 30 Mar 2021.

Trans. Ind. Ceram. Soc., vol. 80, no. 1, pp. 60-63 (2021).

ISSN 0371-750X (Print), ISSN 2165-5456 (Online)
http://dx.doi.org/10.1080/0371750X.2021.1871647

# Effect of Zr/Ti Ratio on Piezoelectric and Dielectric Properties of $0.1Pb[Fe_{1/2}Nb_{1/2}]O_3$-$0.9Pb[Zr_xTi_{(1-x)}]O_{30}$ Ceramics

Louanes Hamzioui,[a, b, *] Fares Kahoul,[a, b] Abdrazek Guemache,[a] Michel Aillerie,[c, d] Ahmed Boutarfaia[b]

[a]Université de M'Sila, Département Socle Commun ST, Faculté de Technologie, M'Sila 28000 Algérie
[b]Université de Biskra, Département de Chimie, Laboratoire de Chimie Appliquée, Biskra 7000 Algérie
[c]Université de Lorraine, LMOPS, EA 4423, 57070 Metz, France
[d]Centrale Supelec, LMOPS, 57070 Metz, France

[MS received May 31, 2020; Revised copy received November 05, 2020; Accepted December 14, 2020]

**ABSTRACT**

**This study describes the microstructure, crystal structure, dielectric and piezoelectric behavior of $0.1Pb[Fe_{1/2}Nb_{1/2}]O_3$-$0.9Pb[Zr_xTi_{(1-x)}]O_3$ ($x$ = 0.49-0.55) ceramics synthesized by solid-state reaction. Compositions were sintered at 1180°C for 120 min. Dense and uniform microstructure was seen through microstructural analysis. XRD pattern confirmed the co-existence of tetragonal and rhombohedral perovskite phases in these compositions where $0.51 \leq x \leq 0.53$. Compositions with $0.51 \leq x \leq 0.53$ resulted in the optimum values of properties, viz. dielectric constant ($\varepsilon_r$) of 1150, piezoelectric coefficient ($d_{31}$) of $95\times10^{-12}$ C/N, piezoelectric voltage constant ($g_{31}$) of $70\times10^{-3}$ mV/N and the coupling factor ($k_p$) value of 0.67. Results indicated that this material composition could be suitable for power harvesting and sensor applications.**

**[Keywords: MPB, Piezoelectricity, Ceramics, Dielectric properties, X-ray methods]**

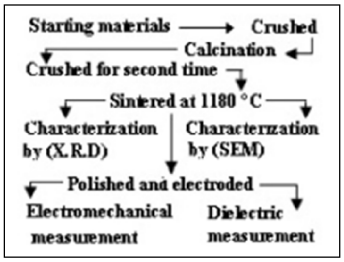


## Introduction

Lead zirconate titanate (PZT) ceramics with general chemical formula $Pb(Zr_xTi_{(1-x)})O_3$ have been extensively studied because of their favourable characteristics.[1–4] Especially, the solid solution composition located near the rhombohedral (antiferroelectric $PbZrO_3$)-tetragonal (ferroelectric $PbTiO_3$) morphotropic phase boundary (MPB, ≈0.5), depending on Zr/Ti ratio, possesses eminent piezoelectric characteristics.[5–10] Lead based ferroelectrics have been in great demand because of their outstanding dielectric and piezoelectric properties which make them suitable for applications like multilayer capacitors, micro-electro mechanical systems (MEMS) and integrated devices such as ferroelectric memories, infrared sensors, micro actuators, etc. Among these materials, $Pb(Zr_xTi_{1-x})O_3$ system and its modified solid solutions are among the most promising materials for piezoelectric applications.[11–14]

Classically, the electrical properties of PZT ceramics are modulated by the addition of a small quantity of cations (typically 0.5-2 mol%). Modification of PZT at $Pb^{2+}$ and $Zr^{4+}/Ti^{4+}$ sites with sufficient substitutions of single or multiple cations helps to improve its physical and electrical properties. Two main types of dopants exist:[15–17] (i) 'Donor' dopants, such as $La^{3+}$, $Nb^{5+}$, $Ce^{3+}$ and $Ta^{5+}$, which produce 'soft' PZT, resulting in the following changes in PZT characteristics: higher dielectric constant and losses (at room temperature), much lower $Q_m$ mechanical efficiency factor, higher $d_{31}/d_{33}$ load coefficient and simple mechanical stress depolarization; lead vacancies compensate for the excess of positive charge in soft PZT. (ii) 'Acceptor' dopants, such as $K^+$, $Na^+$, $Sc^{3+}$ and $Fe^{3+}$, which produce 'hard' PZT, inducing the following changes in PZT characteristics: lower $d_{33}$, lower dielectric constant and losses (at room temperature), much higher mechanical $Q_m$ and difficult mechanical stress depolarization; the loss of a positive charge in hard PZT is offset by vacancies in oxygen. It is anticipated that the dynamic doping of two or more elements combines the properties of donor doped and/or acceptor doped PZT, which could exhibit better stability or improved piezoelectric and dielectric properties than those of the single element doped by PZT.[18–22]

The objective of the present work is to study the effect of Zr/Ti ratio on structural, piezoelectric and dielectric properties of $0.1Pb[Fe_{1/2}Nb_{1/2}]O_3$-$0.9\,Pb[Zr_xTi_{(1-x)}]O_3$ with $x$ = 0.49-0.55. In this paper, an effort has been made to determine the MPB phase contents with variations in the Zr/Ti ratio.

## Experimental

The specimens were manufactured by using a conventional mixed oxide process. The study was carried out on the system $0.1Pb[Fe_{1/2}Nb_{1/2}]O_3$-$0.9Pb[Zr_xTi_{(1-x)}]O_3$ (hereafter named as PFN-PZT) with varying $x$ ($49\% \leq x \leq 55\%$) and a step of $x$ = 2%. The starting materials, viz. $Pb_3O_4$ (99.9%; M/s Aldrich chemicals, USA), $TiO_2$ (98.9%; M/s Travancore Titanium Products), $ZrO_2$ (99.9%;

*Corresponding author; email: louanes.hamzioui@univ-msila.dz

M/s Aldrich Chemicals, USA), $Nb_2O_5$ (99.6%; Biochem) and $Fe_2O_3$ (98%; Acros), were mixed in acetone medium by using a magnetic stirrer for 2 h. The obtained paste was dried at 80°C in a drying oven for 2 h, and then crushed in a glass mortar for 6 h. After crushing, the obtained powder was compacted in the form of pastilles with a pressure of 300 kg/cm$^2$. Then, a preliminary calcination at 800°C was carried out for 2 h with a heating rate of 2°C/min. The calcined mixture was crushed for a second time for 4 h, and pressed into discs of 10 mm diameter and ~1 mm thickness at 200 MPa. The samples were then sintered at 1180°C for 2 h in a covered alumina crucible. To prevent the evaporation of PbO from the pellets, a powder of $PbZrTiO_3$ was used as the embedding powder.

For phase characterization, powder X-ray diffraction (XRD) measurements were carried out using a Rigaku X-ray diffractometer with CuK$\alpha$ radiation. XRD patterns were recorded at a scan rate of 2°/min for 2$\theta$ varying from 30° to 60°. Bulk densities of the sintered ceramics were determined by the Archimedes method.

The sintered PFN-PZT specimens were polished and electroded with silver paste and poled. The piezoelectric constant ($d_{31}$) and electromechanical planar coupling factor ($k_p$) were calculated by using resonance-antiresonance technique using another impendence analyzer (SI1260 Impedance/Gain-Phase Analyzer; Solartron, UK): $k_p = [2.51(f_a–f_r)/f_r)]^{1/2}$, where $f_r$ and $f_a$ are the resonance and antiresonance frequencies, respectively.[23] Zr/Ti ratio dependent dielectric constant ($\varepsilon_r$) and tangent loss (tan$\delta$) were obtained at 1 kHz using an inductance capacitance resistance meter (LCR meter 800 series).

## Results and Discussion

Densities of the samples containing different amounts of Zr/Ti ratio were measured, and the results are shown in Fig. 1. As seen, the densities of the ceramics were in the range of 7.52-7.67 g.cm$^{-3}$ (94-97% theoretical density) and dependent on Zr/Ti ratio. With increasing Zr/Ti ratio, the density of the samples was increased, achieved the highest value (7.67 g.cm$^{-3}$) at the ratio of 51/49, and then decreased. This may be explained from the micro-structures of the ceramic samples.

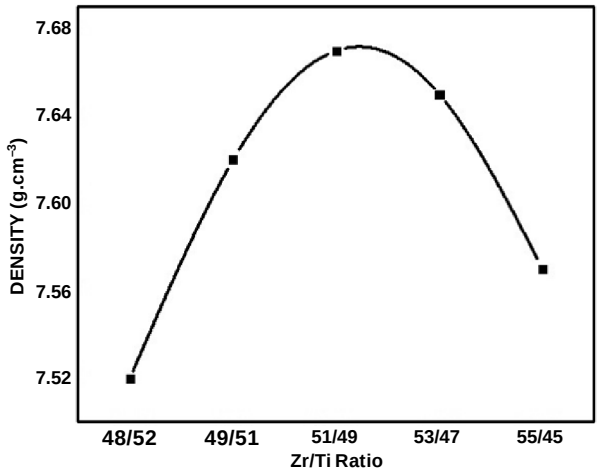


**Fig. 1 – Variation of density of PFN-PZT samples sintered at 1180°C as a function of Zr/Ti content**

Figure 2 shows the SEM images of PFN-PZT ceramics sintered at 1180°C with different Zr/Ti ratios. The figure shows that the microstructures are dense and uniform. When the amount of Zr/Ti ratio increased, the ceramic samples became more dense, and at Zr/Ti = 51/49, a thick and uniform microstructure with a minimal porosity was observed (Fig. 2a); the ceramic sample was almost fully dense for the Zr/Ti ratio of 51/49. The grain size was distributed widely up to 3 μm for Zr/Ti ratios of 51/49 and 53/47. For Zr/Ti ratio of 55/45 porosity was increased. Overall, it was noted that grain growth was encouraged as the Zr/Ti ratio was increased. The quality of the material increased with increasing density and with increasing sintering temperature.[24]

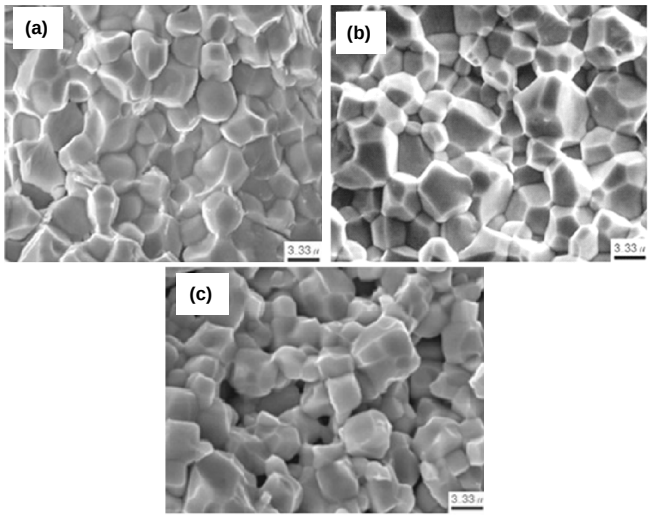


**Fig. 2 – SEM images of the specimens sintered at 1180°C with Zr/Ti ratio of: (a) 51/49, (b) 53/47 and (c) 55/45**

XRD patterns of PFN-PZT ceramics sintered at 1180°C with varying Zr/Ti ratios (51/49, 53/47 and 55/45) are shown in Fig. 3. The presence of sharp and well-defined peaks indicates the presence of a pure perovskite phase with a good degree of crystallinity and no secondary phase formation. Tetragonal and rhombohedral phases were identified by analysis of (002) and (200) peaks in the 2$\theta$ range of 43°-47°.[25, 26] The splitting of (002) and (200) peaks indicates ferroelectric tetragonal phase, while the single (200) peak indicates ferroelectric rhombohedral phase. Triplet peak indicates that the samples consist of a mixture of tetragonal and rhombohedral phases. It can be observed from the XRD pattern that mixtures of tetragonal and rhombohedral phases were formed at Zr/Ti = 51/49 and 53/47 (Figs. 3a and 3b), and rhombohedral phase was identified when Zr/Ti was increased to 55/45 (Fig. 3c).

Figure 4 shows the effect of Zr/Ti ratio on the dielectric properties. It can be observed that by increasing the Zr/Ti ratio, dielectric constant ($\varepsilon_r$) was increased and dielectric loss (tan$\delta$) was reduced. $\varepsilon_r$ went from 550 to 1150 as the

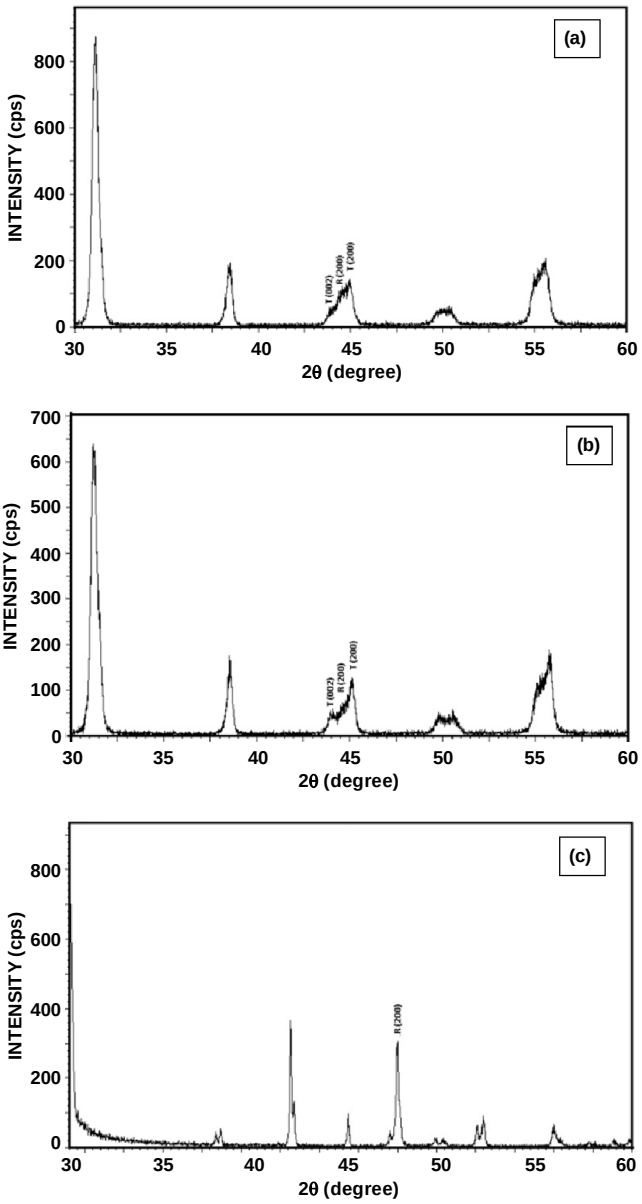


**Fig. 3 – XRD patterns of the specimens sintered at 1180°C with Zr/Ti ratio of: (a) 51/49, (b) 53/47 and (c) 55/45**

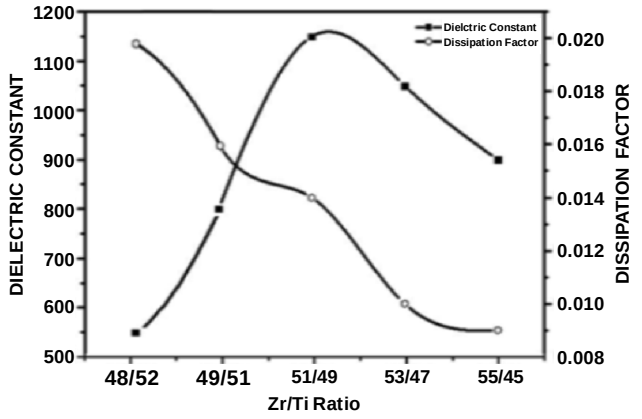


**Fig. 4 – $\varepsilon_r$ and tanδ of PFN-PZT samples sintered at 1180°C as a function of Zr/Ti ratio**

ratio was increased from 48/52 to 51/49. It indicates that as Zr/Ti ratio was increased, the charge storing capacity was increased for PFN-PZT. $\varepsilon_r$ (=1150) was maximum for Zr/Ti = 51/49. This maximum dielectric constant can be explained by the presence of several directions of spontaneous polarization related to the existence of two structures, rhombohedral and tetragonal. However, further increase of Zr/Ti ratio above 51/49 led to gradual reduction of $\varepsilon_r$, most likely due to the change of crystal structure of the materials from MPB to rhombohedral, as shown in Fig. 3. Friction between the domain walls, represented by tanδ, showed decreasing trend with increasing Zr/Ti ratio; tanδ was reduced from 0.02 to 0.009 as Zr/Ti ratio was increased from 48/52 to 55/45.

The change in microstructure and Zr/Ti ratio also affects the piezoelectric properties of PFN-PZT ceramics. Figure 5 shows the variation of $k_p$ and $Q_m$ as a function of Zr/Ti ratio. It is observed from Fig. 5 that as the Zr/Ti ratio increases, value of $k_p$ increases initially, reaching a peak of 0.67 at Zr/Ti ratio of 51/49, and then decreases with further increase of Zr/Ti ratio. $Q_m$ shows an opposite trend of $k_p$ and continues to decrease initially with increasing Zr/Ti ratio, attains a minimum value for Zr/Ti ratio of 51/49, and then increases with further increase of Zr/Ti ratio. This is due to the fact that the phase structure of PFN-PZT ceramics changes from the coexistence of tetragonal and rhombohedral phases to single rhombohedral phase, with the increase of Zr/Ti ratio. Namely, it approaches the morphotropic phase boundary (MPB) when Zr/Ti ratio is 51/49, where the sample obtained a dense and uniform structure. Maximum polarizability resulted into minimum $Q_m$ and maximum $k_p$.

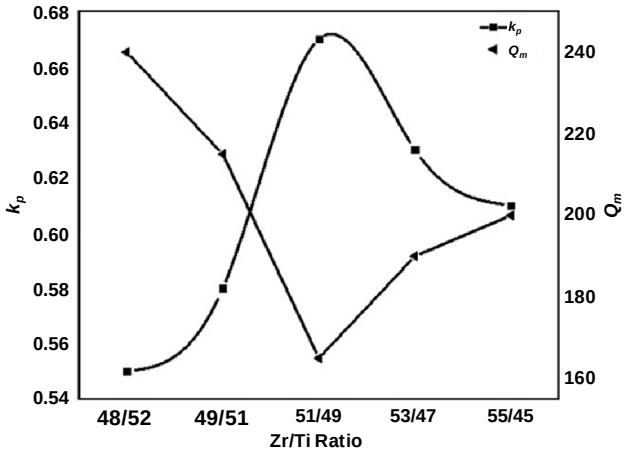


**Fig. 5 – $k_p$ and $Q_m$ of PFN-PZT samples sintered at 1180°C as a function of Zr/Ti ratio**

Figure 6 shows the piezoelectric properties variation ($d_{31}$ and $g_{31}$) with Zr/Ti ratio. Values of $d_{31}$ and $g_{31}$ were enhanced with the increase in the ratio of Zr/Ti until 51/49. At this ratio, the optimum value of $d_{31}$ ($95\times10^{-12}$ C/N) was obtained. This was due to the decrease in porosity. The presence of pore reduced polarization by unit volume, contributing to decrease in $d_{31}$.[27] As the ratio

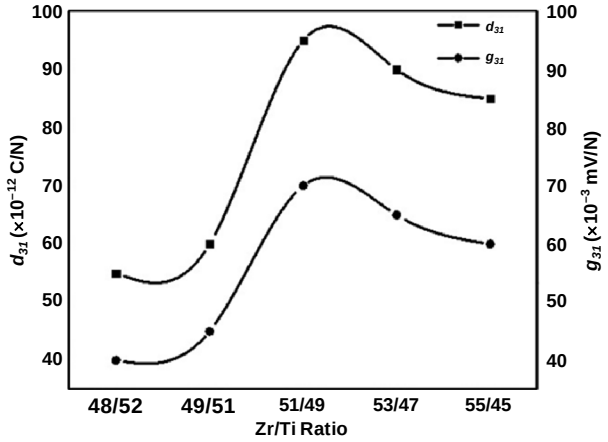


**Fig. 6 – $d_{31}$ and $g_{31}$ of PFN-PZT samples sintered at 1180°C as a function of Zr/Ti ratio**

of Zr/Ti increased further to 55/45 in stages, $d_{31}$ was reduced due to increase in porosity. $g_{31}$ was directly proportional to $d_{31}$ and was optimal ($70\times10^{-3}$ mV/N) for the Zr/Ti ratio of 51/49.

## Conclusions

A series of $0.1Pb[Fe_{1/2}Nb_{1/2}]O_3$-$0.9Pb[Zr_xTi_{(1-x)}]O_3$ ceramics ($x$ = 0.49, 0.51, 0.53 and 0.55) were synthesized by conventional mixed-oxide ceramic processing technique. Results of this study are summarized as follows:

- X-ray diffraction analyses indicated a pure solid solution of PFN-PZT without any second phase. X-ray diffraction studies also revealed that PFN-PZT with 0.51 and 0.53 showed a MPB region.
- At the Zr/Ti ratio of 51/49 and sintering temperature ($T_s$) of 1180°C, the density, electromechanical coupling factor ($k_p$), dielectric constant ($\varepsilon_{max}$), piezoelectric constant ($d_{31}$), dielectric loss ($\tan\delta$) and mechanical quality factor ($Q_m$) showed the optimum values of 7.67 g.cm$^{-3}$, 0.67, 1150, 95 pC/N, 0.009 and 165, respectively. Therefore, they can be a promising material for using in high power piezoelectric devices.

### References


1. J. Y. Ha, J. W. Choi, C. Y. Kang, D. J. Choi, H. J. Kim and S. J. Yoon, *Mater. Chem. Phys.*, **90**, 396-400 (2005).
2. J. S. Cross, K. Shinozaki, T. Yoshioka, J. Tanaka, S. H. Kim, H. Morioka and K. Saito, *Mater. Sci. Eng. B*, **173**, 18-20 (2010).
3. A. Ballato, *IEEE Trans. Ultrason. Ferroelectr. Freq. Control*, **42**, 916-926 (1995).
4. C. T. Lin, B. W. Scanlan, J. D. Mcnell, J. S. Webb and L. Li, *J. Mater. Res.*, **7**, 2546-2554 (1992).
5. R. Sagar, S. Madolappa and R. L. Raibagkar, *Trans. Indian Ceram. Soc.*, **70**, 131-134 (2011).
6. Z. Xing, L. Jin, Y. Feng and X. Wei, *J. Electron. Mater.*, **43**, 2614-2620 (2014).
7. V. Porokhonskyy, L. Jin and D. Damjanovic, *Appl. Phys. Lett.*, **94**, 212906 (2009).
8. A. Boutarfaia and E. Bouaoud, *Ceram. Int.*, **22**, 281-286 (1995).
9. L. Jin, V. Porokhonskyy and D. Damjanovic, *Appl. Phys. Lett.*, **96**, 242902 (2010).
10. B. Noheda, J. A. Gonzalo, L. E. Cross, R. Guo, S.-E. Park, D. E. Cox and G. Shirane, *Phys. Rev. B*, **61**, 8687-8695 (2000).
11. D. Yuan, Y. Yang, Q. Hu and Y. Wang, *J. Am. Ceram. Soc.*, **97**, 3999-4004 (2014).
12. B. Keswani, S. Patil and Y. Kolekar, *Trans. Indian Ceram. Soc.*, **78**, 108-110 (2019).
13. S. Zhao, H. Wu and Q. Sun, *Mater. Sci. Eng. B*, **123**, 203-210 (2005).
14. B. R. Kumar, N. V. Prasad, G. Prasad and G. S. Kumar, *Trans. Indian Ceram. Soc.*, **78**, 89-93 (2019).
15. B. Guiffard, E. Boucher, L. Lebrun and D. Guyomar, *Mater. Sci. Eng. B*, **137**, 272-277 (2007).
16. Q. W. Hng and H. Hoon, *Mater. Chem. Phys.*, **75**, 151-156 (2002).
17. I. Lazar, M. A. Habrajska, M. Pawelczyk, M. Górny, A. Zawada and K. Roleder, *J. Electroceram.*, **40**, 203-210 (2018).
18. B. W. Lee and E. J. Lee, *J. Electroceram.*, **17**, 597-602 (2006).
19. V. S. M. Sharma and G. S. Dhami, *Trans. Indian Ceram. Soc.*, **27**, 13N-18N (1968).
20. S. Zahi, R. Bouaziz, N. Abdessalem and A. Boutarfaia, *Ceram. Int.*, **29**, 35-39 (2003).
21. N. Zelikha, B. Ahmed, K. Amel, M. Hayet, B. Karima, A. Malika, A. Nora and M. Abdelhek, *Int. J. Pharm. Biol. Sci.*, **4**, 438-446 (2014).
22. P. Jaita, A. Watcharapasorn and S. Jiansirisomboon, *J. Microsc. Soc. Thailand*, **24**, 21-24 (2010).
23. Z. He, J. Ma and R. Z. Hang, *Ceram. Int.*, **30**, 1353-1356 (2004).
24. A. Boutarfaia, *Ceram. Int.*, **26**, 583-587 (2000).
25. H. Chen, J. Long and Z. Meng, *Mater. Sci. Eng. B*, **99**, 433-436 (2003).
26. H. Chen, X. Guo and Z. Meng, *Mater. Chem. Phys.*, **75**, 202-206 (2002).
27. M. C. Wang, *J. Mater. Sci.*, **37**, 663-668 (2002).